　　http://www.journalmt.com

Experimental Investigation of Armour (Armox-Aramid-UHMWPE)

Jindřich Viliš (0000-0003-1690-8454)[1], Roman Vítek (0000-0003-3177-6015)[1], Jan Zouhar (0000-0001-8031-8366)[2], Michal Stejskal (0000-0002-5733-8278)[3], Vlastimil Neumann (0000-0001-7428-1309)[1]
[1]Faculty of Military Technology, University of Defence in Brno. Kounicova 65, 612 00 Brno. Czech Republic.
E-mail: jindrich.vilis@unob.cz
[2]Faculty of Mechanical Engineering, Brno University of Technology, Technická 2, 616 69 Brno, Czech Republic.
[3]Faculty of Mechanical Engineering, Research Center of Manufacturing Technology, Czech Technical University in Prague, Horská 3, 128 00 Prague 2, Czech Republic.

In this study, the ballistic resistance of multi-layered composite armour is experimentally investigated. The composition of this armour consisted of armour steel Armox 500T, para-aramid fabric Twaron CT 747 and ultra-high molecular weight polyethylene Endumax Shield XF33. To compare the ballistic resistance, the ballistic resistance of the armour with the perforated steel Armox 500T was tested. The rifle cartridges 7.62 x 51 mm FMJ NATO M80 were used to test this resistance. The aim of this experiment was to compare the ballistic resistance of unperforated and perforated steel Armox 500T. As part of the experimental part, the chemical composition and microhardness of the steel Armox 500T was verified. The hardness of the composite materials was also measured for optimal armor configuration. After the projectile impact, the damage mechanism of the steel Armox 500T and the composite materials were investigated by using optical and electron microscopy. It was proved that the ballistic resistance of the perforated steel depends on the used pattern. Based on the performed experiments, the steel Armox with pattern A effectively reduced the weight of the testing configuration and absorbed all the kinetic energy of the projectile 7.62 mm FMJ M80.

Keywords: Ballistic resistance, Armour protection, Perforated sheet, Composite, Aramid

1 Introduction

The operation of international armed forces in peacekeeping operations increases the need to protect military, police and civilian personnel [1]. In terms of design and material solutions, the choice of multi-layered ballistic protection is offered. This is a combination of metal, lightweight metal alloys with composite materials or ceramics with composite materials [2, 3]. The advanced manufacturing technologies and developments in materials engineering make it possible to optimize the structure of ballistic protection to provide ballistic and multihit resistance with minimum area weight. For an individual it would protect the most important organs of the human body, for light military equipment it would allow to protect the most exposed parts of the vehicle against the effects of projectiles, shrapnel or mines and explosives [3, 4, 5, 6].

The modern trend is to gradually replace homogeneous steel armour, which has the same chemical composition in the entire thickness and volume, with multi-layered composite armour [7, 8]. The construction of this armour consists of a strike face layer and a back face layer. For the strike layer, high-strength steels (Armox®, Hardox®, DFNDR Armor® or MARS Armor®) or ballistic ceramics

(Al$_2$O$_3$, SiC, B$_4$C, or their combinations) are most often used. This layer must be hard enough to ensure not only the deceleration and destabilization of the projectile, but also the disruption or fragmentation of its structure [9, 10]. The underlayer is composed of para-aramid (Kevlar®, Twaron®), polyethylene (UHMWPE), glass (E-glass, S-glass), carbon fibre (CFRP) or its combinations for hybridization purposes. It is characterized by high toughness. Its purpose is to absorb the residual kinetic energy of projectile fragments or fragmented strike face layer [11, 12, 13].

In this article, the multi-layered composite armour consisting of high-strength steel Armox 500T and composite panels Twaron CT 747 and Endumax Shield XF33 was designed, fabricated and ballistically tested. The ballistic resistance of the designed armour was tested by the cartridges 7.62 x 51 FMJ NATO M80 with lead-core projectile and the ballistic resistance verification was performed in accordance with STANAG AEP-55 NATO, level 1. To reduce the area weight of the multi-layered composite armour, the ballistic resistance of the perforated Armox steel 500T was compared. Furthermore, verification of the chemical composition, microhardness measurements, and evaluation of the microstructure and fractography of steel Armox 500T

　　　　　indexed on http://www.webofscience.com and http://www.scopus.com

were performed. The hardness of the composite materials was measured to determine the optimum test configuration. After ballistic testing, the damage mechanism of the composite materials was evaluated. Based on these experimental methods, the information obtained can be used to effectively develop a high-performance multi-layered composite armour.

2 Materials and methods

Ballistic materials must be able to resist the effects of projectiles or shrapnel of different geometries that are accelerated to different velocities. They must also be able to resist the force effects generated by the detonation of explosives [1, 5].

High-strength steel Armox 500T and composite materials: para-aramid fabric Twaron CT 747 and ultra-high molecular weight polyethylene Endumax Shield XF33 were used to create the multi-layered composite armor.

Steel Armox® is the high-strength low-alloy steel supplied by the Swedish company SSAB Oxelösund in various modifications according to specific needs. The most widely used modifications include Armox 440T, Armox 500T and Armox 600T. The different modifications are characterized by the amount of alloying additives, the heat treatment and a numerical value that indicates the average Brinell hardness. A higher number guarantees higher hardness and tensile strength, but at the same time there is a decrease in toughness, ductility and weldability [2, 9, 14, 15].

Para-aramid fibres are synthesized from 1,4-phenylene diamine monomer and terephthaloyl chloride to form hydrochloric acid. This synthesis produces an aramid containing benzene nuclei and amide groups. By further modifications, the polymer chains are oriented according to the axis of the fibre.

The main advantages of these fibres are their high strength and stiffness, which are due to the regular arrangement of phenylene nuclei and amide groups with hydrogen-bridge bonds. In addition to high strength and stiffness, they are characterized by a high modulus of elasticity, excellent dimensional stability and high resistance to fire and chemicals. At temperatures above 400 °C they do not burn, but only carbonize, which does not support further burning. Para-aramid fibres also have their disadvantages, which include low compressive strength compared to tensile strength and degradation by alkaline acids and UV radiation. The most well-known representatives of para-aramids include Kevlar® and Twaron® [5, 7, 12, 16].

Ultra-high molecular weight polyethylene UHMWPE is formed by softening a gel of polyethylene with an extremely high molecular weight, which ranges from 4 000 000 g/mol to 8 000 000 g/mol. Due to the high viscosity of the melt, processing by conventional processes such as injection moulding or extrusion is not possible. The polyethylene gel is softened in a decalin water bath. In the precipitation bath, a network of chains is formed which can be lengthened several times. This high molecular weight gives rise to a highly oriented structure which gives the fibres high strength. These fibres have high resistance to surface abrasion, resistance to UV degradation, resistance to most chemicals, low moisture absorption and low coefficient of friction. This type of polyethylene is better known by the trade names Dyneema®, Spectra® or Endumax® [5, 7, 12, 17, 18].

The high-strength armour steel Armox 500T and the composite materials Twaron CT 747 and Endumax Shield XF33 that were used to create the multi-layered composite armour are shown in Fig. 1.
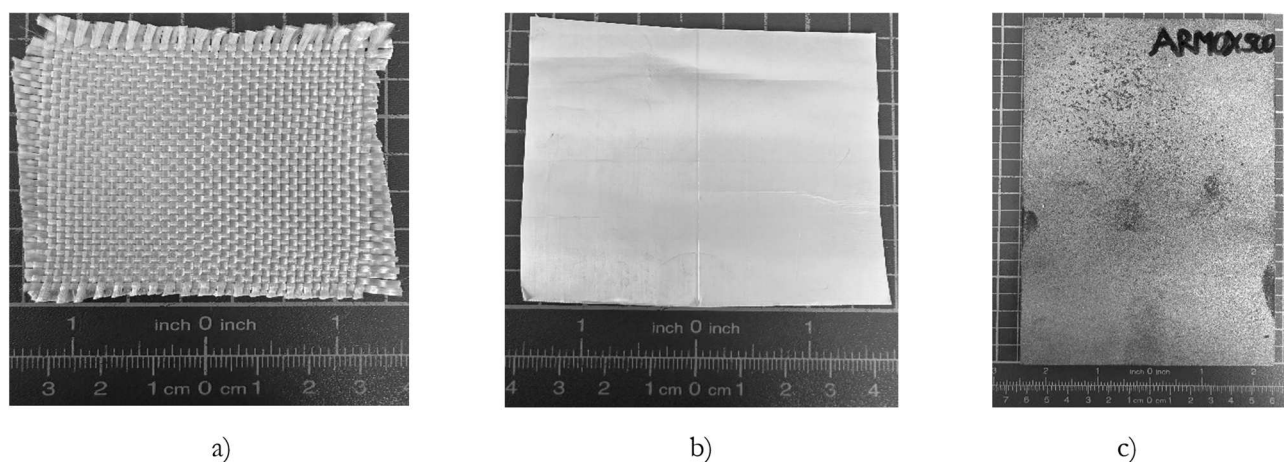

a)   b)   c)

Fig. 1 *Selected materials for multi-layered composite armour: a) Twaron CT 747; b) Endumax Shield XF33; c) Armox 500T*

Selected material properties of the para-aramid fabric Twaron CT 747 and ultra-high molecular weight polyethylene Endumax Shield XF33, as specified by the manufacturer [19, 20], are shown in Tab. 1. Selected properties and chemical composition of steel Armox 500T are given in Tab. 2.

Tab. 1 *Selected properties of the composite materials Twaron CT 747 and Endumax Shield XF33 [19, 20]*

Materials	Thickness [mm]	Area density [g/m^2]	Tensile strength module [GPa]	Composite density [kg/m^3]
Twaron CT 747	0.62	410	115	1450
Endumax Shield XF33	0.16	146	170	970

Tab. 2 *Selected properties and chemical composition of steel Armox 500T [21]*

Armox 500T	Chemical composition [wt. %]	Hardness [HBW]	Tensile strength R_m [MPa]	Yield strength $R_{p0.2}$ [min MPa]	Ductility A_5 [min %]
Datasheet	C (0.32); Si (0.40); Mn (1.2); P (0.010); S (0.003); Cr (1.0); Ni (1.8) B (0.005);	480–540	1450–1750	1250	8

2.1 Ballistic composite processing technology and preparation of perforated sheet Armox 500T

Currently, composites can be manufactured by using various technologies. Depending on the type of reinforcement and matrix used, the required temperature for curing the resin, the desired shape of the components and the production costs, it is necessary to select the appropriate production technology [5, 22, 23]. In this section, two basic composite processing technologies are described more detailed: Vacuum Assisted Resin Transfer Moulding (VARTM) and hot pressing.

VARTM technology is the closed method. It is the modification of the classical RTM technology in which the upper part of the form is replaced by a vacuum foil and the vacuum is used to impregnate the supporting reinforcement. The use of vacuum allows the flow of matrix into the support reinforcement more easily. Based on the created vacuum, impregnation of the support reinforcement is achieved, which minimizes the amount of unwanted air bubbles. The impregnation is followed by curing of the composites, which are cured at room temperature. This technology allows the possibility of constructing less robust forms and therefore offers the advantage of producing large composite parts [5, 22].

Hot pressing is performed at increased temperatures and pressures in two or multipart metal forms that are heated by electric or heating media. These forms are then placed in hydraulic presses. The starting material for this technology is prepregs, which are in the form of SMC (Sheet moulding compound), DMC (Dough moulding compound) or BMC (Bulk moulding compounds). A hydraulic press is used to form the materials into a metal form and the prepreg is cured due to the increased temperature and pressure. This technology allows for a shorter production cycle and is therefore the most productive technology in the high-volume production of small and medium-sized composite parts [5, 23].

VARTM technology was used to produce ballistic composite panel A, which consisted of the support reinforcement in the form of dry para-aramid Twaron CT 747 fabric and the matrix LG700 + HG700. After cutting, stacking the fabric with the required number of layers, this fabric was vacuumed. The matrix was used to impregnate the dry para-aramid fabric, which consisted of the epoxy resin LG700 and the curing reagent HG700 at the ratio of 10:3. The curing process took 24 hours at room temperature of 22 °C. The deposition of the para-aramid fabric, preparation for vacuuming and curing is shown in Fig. 2.
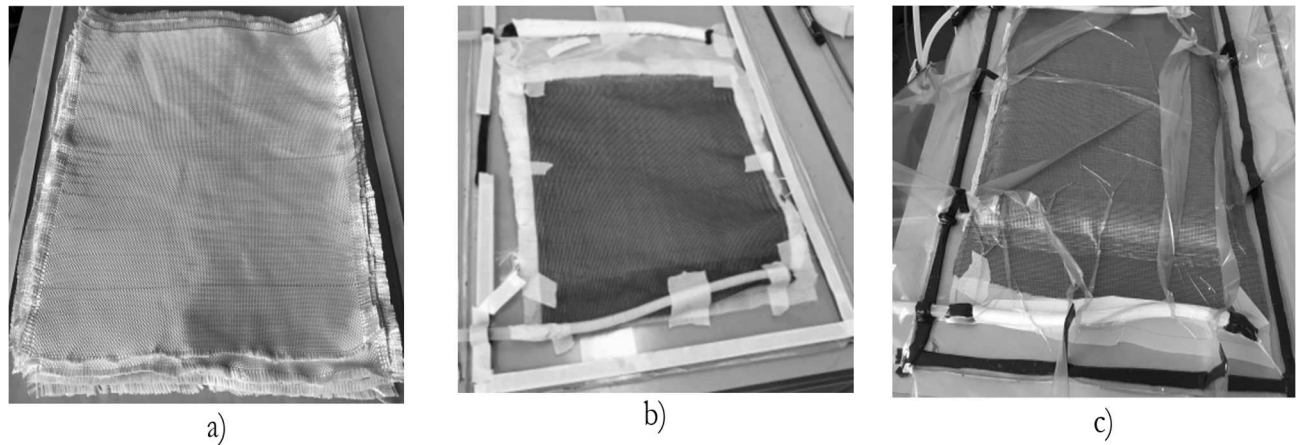
***Fig. 2** Process of production of composite panel A by VARTM technology: a) cut and layered fabric Twaron CT 747; b) preparation for VARTM method; c) curing of matrix LG700 + HG700*

Ballistic composite panels B and C were produced by hot pressing method. Ballistic composite panel B was made of para-aramid fabric Twaron CT 747 impregnated with thermoplastic resin TH110 and ballistic composite panel C was made of ultra-high molecular weight polyethylene Endumax Shield XF33. The pressing process of the panels was performed on the hydraulic press ZD40 with a maximum loading force of 400 kN. The machine with the loading force of 300 kN was applied to panel B for 20 minutes. Panel C was loaded with 350 kN for 20 minutes. The curing temperature for panels B and C was fixed at 140 °C. After the time had passed, the controlled cooling to 80 °C was followed. The preparation of the composite materials and panel production on the ZD40 hydraulic press is shown in

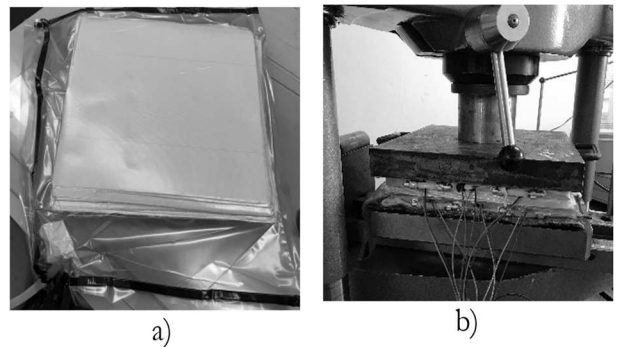Fig. 3. The pressing processes for ballistic composite panels B and C are shown in Fig. 4.

***Fig. 3** Hot pressing technology: a) preparation of composite materials; b) pressing on hydraulic press ZD40*

—●— Pressing temperature Twaron CT 747 TH110 [°C]
—●— Pressing force Twaron CT 747 TH110 [kN]

—●— Pressing temperature Endumax [°C]
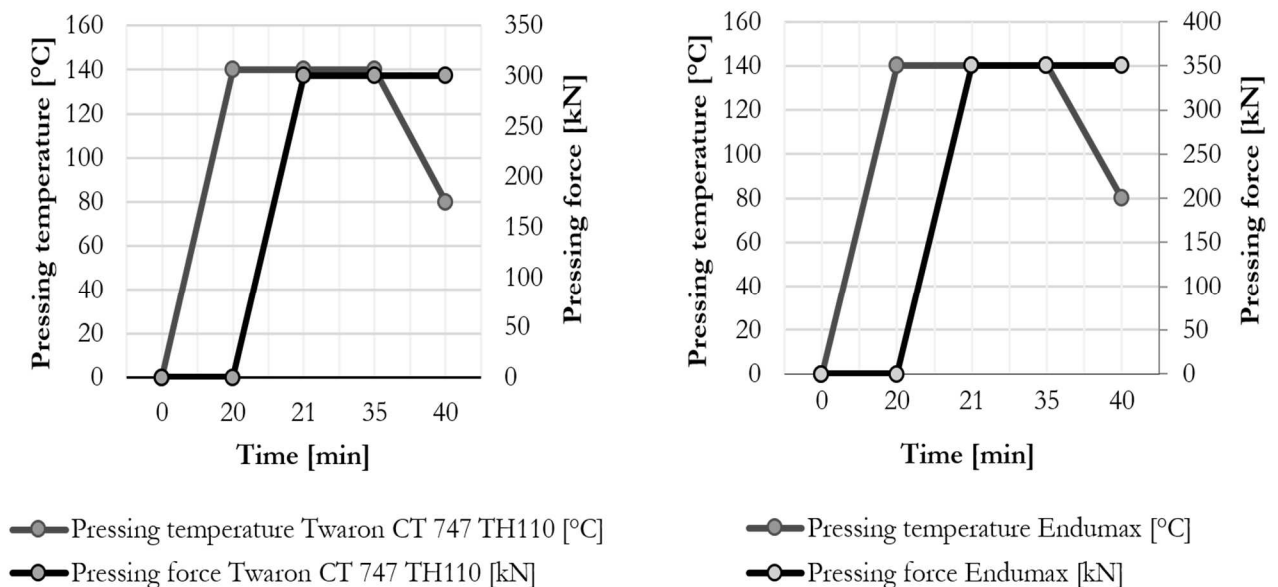—●— Pressing force Endumax [kN]

***Fig. 4** The pressing processes for ballistic composite panels B and C*

After the curing, the ballistic composite panels A, B and C were subsequently cut to the required dimensions of 300 x 300 mm by using the abrasive

waterjet. The basic parameters of the cut ballistic composite panels A, B and C are shown in Tab. 3.

**Tab. 3** *The basic parameters of ballistic composite panels A, B and C*

Ballistic composite panel	Materials	Thickness [mm]	Weight [g]	Number of layers
A	Twaron CT 747 LG700 + HG700	5.1	0.59	10
B	Twaron CT 747 TH110	17.2	1.52	35
C	Endumax Shield XF33	5.6	0.44	35

To increase the ballistic resistance, the composite panels were reinforced with two armoured non-perforated sheets Armox 500T with the thickness of 6.5 mm and dimensions of 200 x 120 mm. In order to reduce weight, one armoured sheet was perforated by using the carbide drill Coro Drill 460. For the drilling of pattern A and pattern B, the CNC centre MCU 700V-5X Rapid was used and the following cutting conditions were chosen:

- cutting speed v_c = 22 m.min^{-1}

- speed n = 1400 min^{-1}
- feed f = 0.05 mm·rev^{-1}
- central cooling by oil emulsion

The total of 254 through holes were drilled in the triangular configuration with the angle of 60°. For pattern 1, 145 holes were drilled with the diameter of 5 mm and the spacing of 8 mm. For pattern 2, 109 holes of 5 mm diameter with the spacing of 11 mm were drilled. The designed and manufactured patterns are shown in Fig. 5.
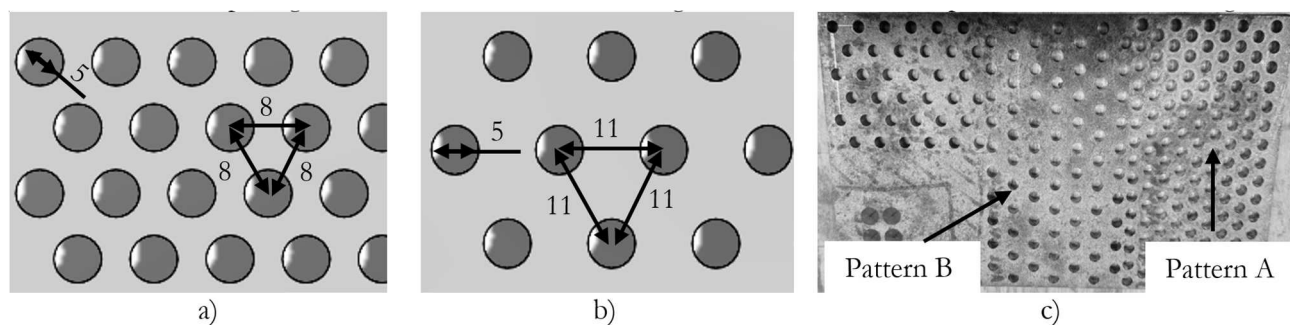
Fig. 5 *Designed patterns of Armox 500T: a) pattern A; b) pattern B; c) manufactured perforated sheet Armox 500T*

2.2 Determination of selected material characteristic of the used materials

In terms of evaluating the usability of selected materials for the design of multi-layered armour, it is necessary to determine the basic material characteristics by which ballistic resistance can be predicted. For metallic materials these are yield strength, ultimate strength, ductility, toughness and hardness. For composite materials, it is the determination of ultimate tensile strength, ultimate breaking strength, hardness, ultimate ductility and

breaking ductility. High ballistic resistance is conditioned by high values of strength and hardness, which results in decreasing toughness and the development of brittle failure. Due to these opposing properties, an acceptable compromise between optimum strength and toughness is chosen [1, 5].

To verify the chemical composition of the steel Armox 500T, the spark spectrometer Q4 TASMAN was used. Tab. 4 shows the elemental concentration values verified by the spark spectrometer Q4 TASMAN.

Tab. 4 *Chemical composition of Armox 500T verified by the spark spectrometer Q4 TASMAN*

Armox 500T	C	Si	Mn	P	S	Cr	Ni	Mo	B
Q4 TASMAN	0.224	0.276	0.881	0.005	0.002	0.774	0.902	0.334	0.001

Microhardness of steel Armox 500T were performed by using a Vickers indenter, which allows force loads ranging from 0.9807 N to 9.807 N. To identify the hardness in the thickness direction of this steel, the semi-automatic microhardness tester Leco M 400 was used [21].

To determine the hardness of composite materials, the Shore D method was used. This is a dynamic hardness testing method, the principle of which is to

press a cone-shaped test specimen with a peak angle of 30° into a test sample with a minimum thickness of 6 mm. For this method, the prescribed test load of 49.03 N must be observed. In the case of hardness measurements of non-metallic materials, it is necessary to observe the prescribed loading time compared to metallic materials, due to the occurrence of permanent deformations and the possibility of distortion of the measured values [22].

For the purpose of microstructural characterization, specimens were cut from the high-strength steel Armox 500T by using the metallurgical saw Leco Viper. The specimens were pressed into the thermoplastic moulding compound Struers Isofast. Subsequently, the specimens were sanded with abrasive papers and polished with a velvet wheel with the diamond polishing paste of 0.5 µm grit. To visualize the desired microstructure, the specimens were etched with the 2% Nital solution. The microstructure of the metallographic specimens Armox 500T, see Fig. 6, and the microstructure of the composite materials Twaron CT 747 and Endumax Shield XF33, see Fig. 7, were observed by using the optodigital microscope Olympus DSX500 and the scanning electron microscope TESCAN MIRA 4.

a)   b)   c)
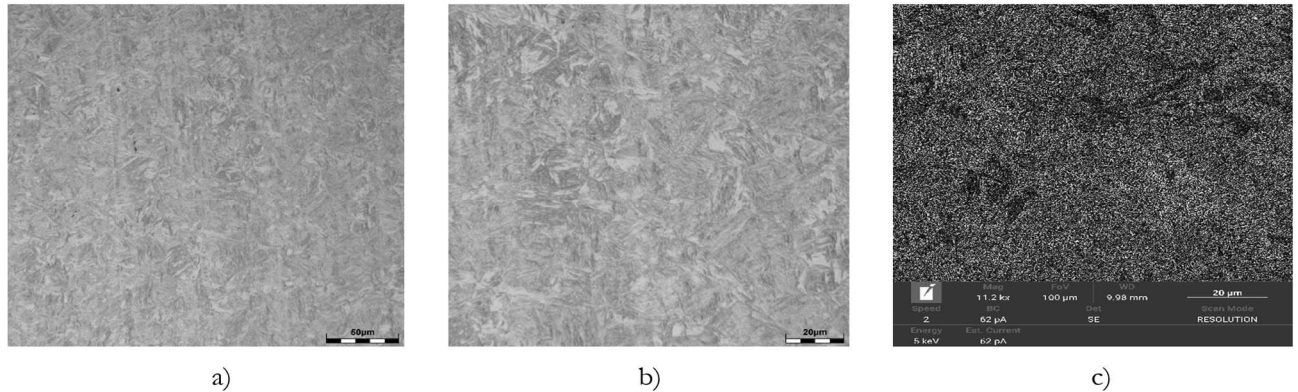
Fig. 6 *Microstructure of Armox 500T: a) microstructure of Armox 500T (optodigital microscopy, magnified 1000x); b) microstructure of Armox 500T (optodigital microscopy, magnified 1000x); c) microstructure of Armox 500T (scanning electron microscopy, magnified 11,000x)*
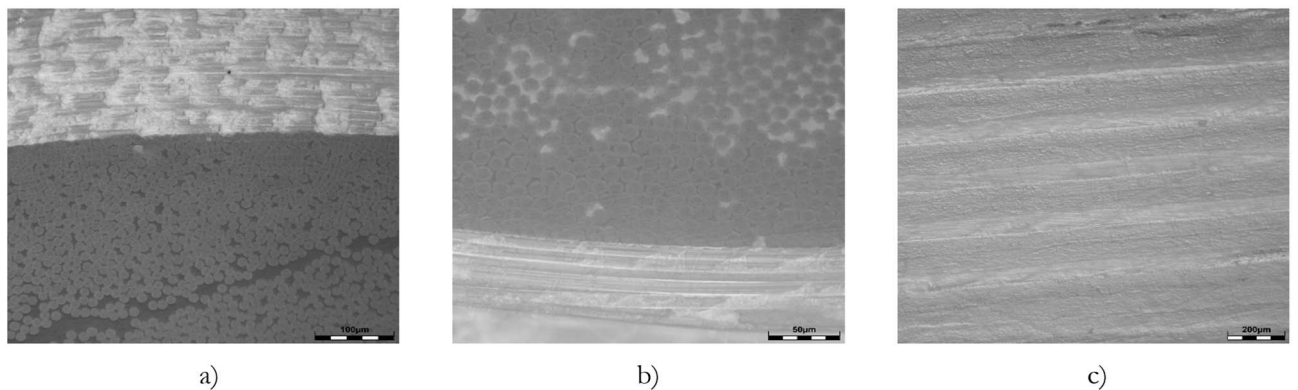

a)   b)   c)

Fig. 44 *Microstructure of composite materials, optodigital microscopy: a) Twaron CT 747 LG700 + HG700 (magnified 500x); b) Twaron CT747 TH110 (magnified 1000x); c) Endumax Shield XF33 (magnified 200x)*
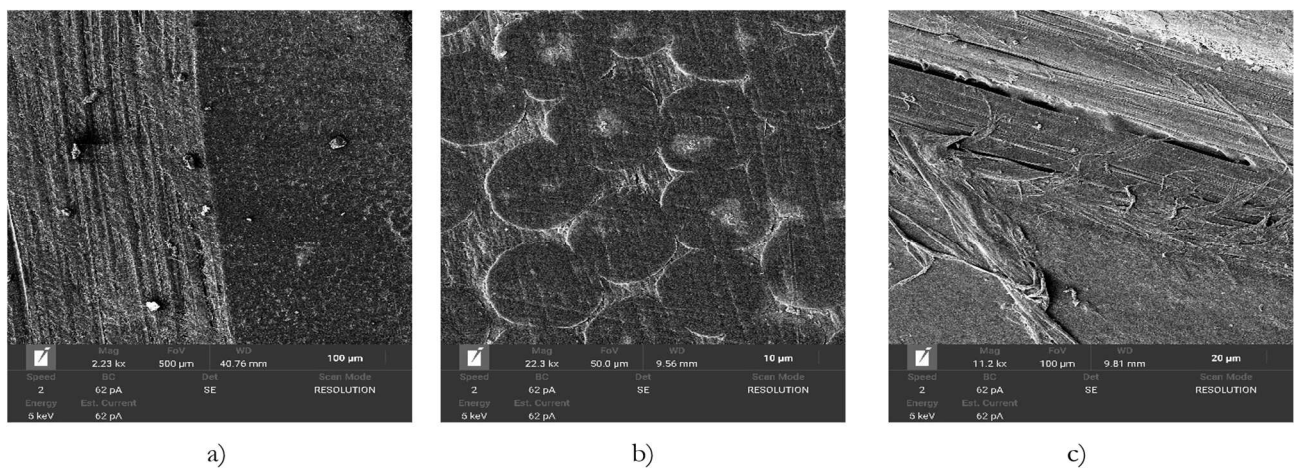

a)   b)   c)

Fig. 45 *Microstructure of composite materials, scanning electron microscopy: a) Twaron CT 747 LG700 + HG700 (magnified 2000x); b) Twaron CT747 TH110 (magnified 22,000x); c) Endumax Shield XF33 (magnified 11,000x)*

Fig. 6 shows that the microstructure of Armox 500T consists of the martensitic-bainitic structure. This microstructure is composed mainly of tempered needle-shaped martensite, with carbides present in the structure, which were formed as conversion products from residual austenite.

The microstructure of para-aramid fabric Twaron CT 747 and ultra-high molecular weight polyethylene is shown in Fig. 7. Fig. 7 and Fig. 8 show cross-sections of the given composite materials.

Fig. 7 and Fig. 8 show that the composition of the para-aramid fabric Twaron CT 747 contained layers arranged at an angle of [0/90] and the composition of the ultra-high molecular weight polyethylene consisted of cross polymer films arranged at an angle of [0/90].

2.3 Shooting experiment

Testing and evaluation of ballistic resistance of protective equipment is related to international and national norms or standards that define methods and parameters for performing ballistic tests. In the context of these norms and standards, these tested devices are divided into ballistic protection of the individual, which is further divided into wearable and non-wearable protective equipment, and ballistic protection of vehicles [1, 5].

To determine the ballistic resistance of these equipment, a number of technical norms and standards are used, depending on their country of origin and ballistic testing requirements.

The most well-known and most widely used standard for testing the ballistic resistance of personal protective equipment is the US National Institute of Justice test NIJ 0101.06. The Czech national technical standard for personal protective equipment is CSN 395360, which is very similar to the US standard NIJ 0101.06. This Czech standard is a comprehensive technical standard that covers ballistic resistance levels, ballistic resistance limits and classes of resistance to stabbing. Another recognized standard used in the Czech Republic is VPAM APR 2006. For the determination of ballistic resistance to shrapnel, CS 130027 is used, which is adopted and translated from the NATO standardization agreement STANAG 2920 [26, 27, 28, 29, 30].

In the context of ballistic resistance evaluation of military vehicles, the STANAG 4569 and AEP-55 standards are in valid. These standards describe the level of protection against kinetic threats in the form of projectiles or shrapnel and also specify the requirements for testing vehicles under the detonation of explosives [31].

The shooting experiment was realized in the ballistic laboratory located at the Faculty of Military Technology, University of Defence, Brno, Czech Republic. The standard STANAG AEP-55 NATO, level 1, was used to estimate the ballistic resistance of the designed armour. The ballistic resistance testing of the armour was performed at the reduced distance of 25 m.

The shooting station included the following configuration of equipment: the shooting bench (Prototype-ZM, STZA 12) connected with the universal breech (Prototype-ZM, UZ-2002) and the exchangeable ballistic barrel (Prototype-ZM, 7. The ballistic radar (Prototypa-ZM, DRS-01) and optoelectronic gate (Kistler, 2521A) were used to measure the velocity of the projectile along the flight trajectory. The ballistic recorder (Kistler, 2519A) was used to record the data. The high-speed camera (Photron, SA-Z) with reflectors was used to visually document the impact of the projectile into the multi-layered composite armour. Fig. 9 shows the used experimental equipment.
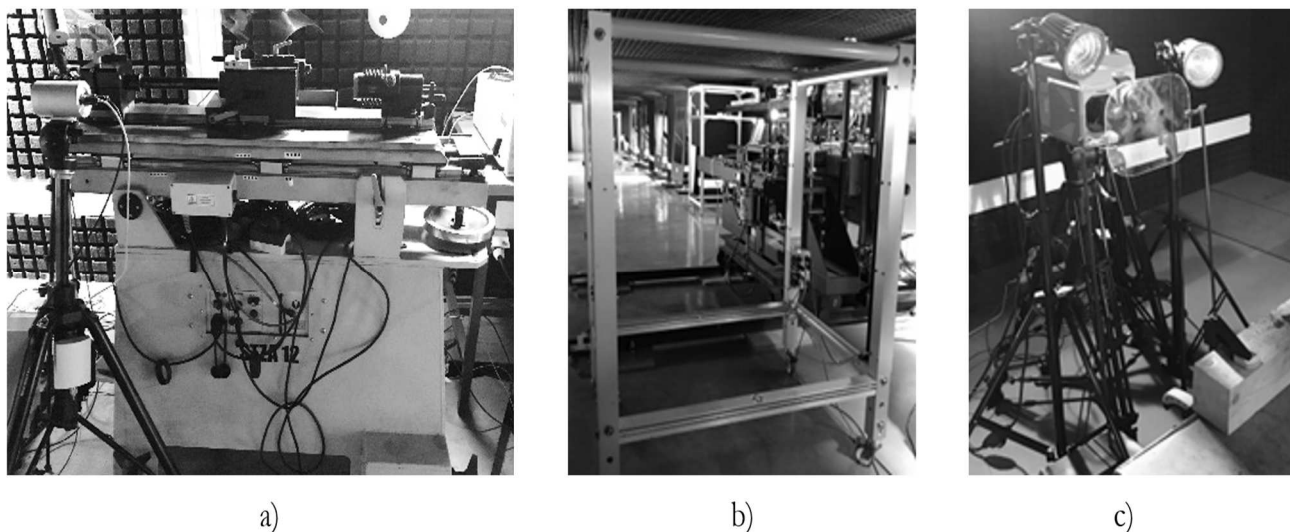

a)   b)   c)

Fig. 9 *Experimental equipment: a) shooting bench, universal breech, exchangeable ballistic barrel and ballistic radar; b) optoelectronic gate; c) high-speed camera with reflectors*

Ballistic testing was performed by the rifle cartridges 7.62 mm x 51 FMJ NATO M80 with the lead core. According to the standard AEP-55, the initial velocity of the projectile is 833±20 m/s and the weight of the projectile is 9.55 g.

3 Results and discussion

This chapter describes the results that were obtained by the discussed experimental methods. In subchapter 3.1, the results of microhardness measurements of the steel Armox 500T and the hardness values of the composite materials Twaron CT 747 and Endumax Shield XF33 are presented. In this subchapter 3.1, the multi-layered composite armour is designed according to the measured hardness values. In subchapter 3.2, the results of ballistic testing are presented and discussed. There is also described in more detail the failure mechanisms of the armour steel Armox 500T and the composite materials Twaron CT 747 and Endumax Shield XF33.

3.1 Microhardness of steel and hardness of composite materials

The microhardness of the steel Armox 500T, which was obtained by the Vickers hardness testing method using the semi-automated microhardness tester Leco M 400 with the load force of 0.49 N, is shown in Fig. 10.
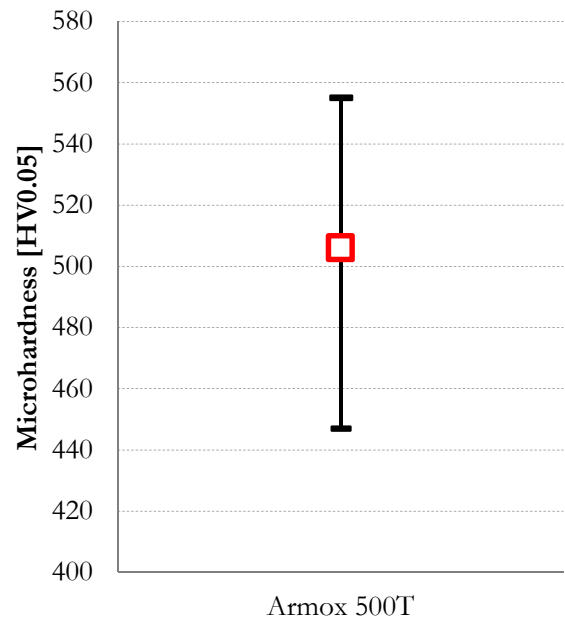

Fig. 10 *Microhardness Armox 500T*

Tab. 5 *Hardness of composite materials*

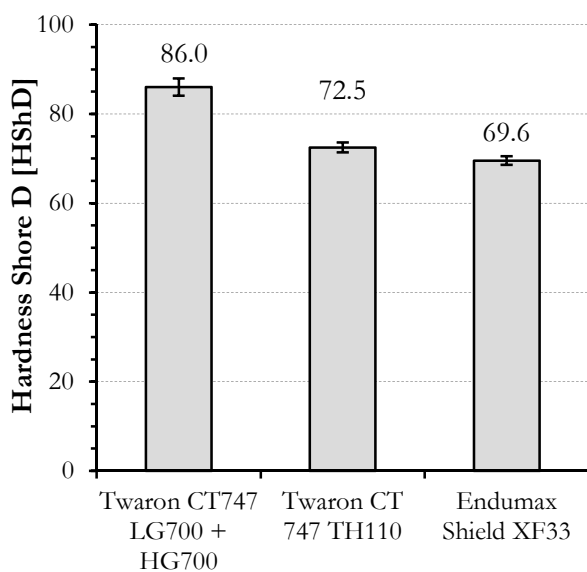| Surface hardness Shore D, num. m.	Twaron CT 747 LG700 + HG700	Twaron CT 747 TH110	Endumax Shield XF33
1	86.7	72.8	70.0
2	86.1	70.9	71.1
3	85.8	73.1	68.8
4	87.3	73.4	69.7
5	84.3	72.3	68.2
Average value	86.0±1.01	72.5±0.88	69.6±1.00

Fig. 11 *Graphical dependence of hardness of composite materials*

The average microhardness value of the steel Armox 500T is 506 HV0.05. The maximum hardness value of this is 555 HV0.05 and its minimum hardness value is 447 HV0.05.

The Shore D hardness of the composite materials was determined by using the hardness tester DIGI-Test II. To determine this value, five measurements were taken for each material and the average value was determined. Tab. 5 and Fig. 11 show the hardness values of the composite materialsFig. 11 shows that the Twaron CT 747 composite material impregnated with thermosetting resin LG700 and curing reagent HG700 demonstrated the highest hardness value. The thermoplastic composite materials Twaron CT 747 TH 110 and Endumax Shield XF33 showed comparable hardness values according to Shore D.

Based on these obtained material properties, the multi-layered composite armour Armox-Aramid-UHMWPE was constructed. The model of the multi-layered composite armour and the location of the armour steel Armox 500T is shown in Fig. 12.
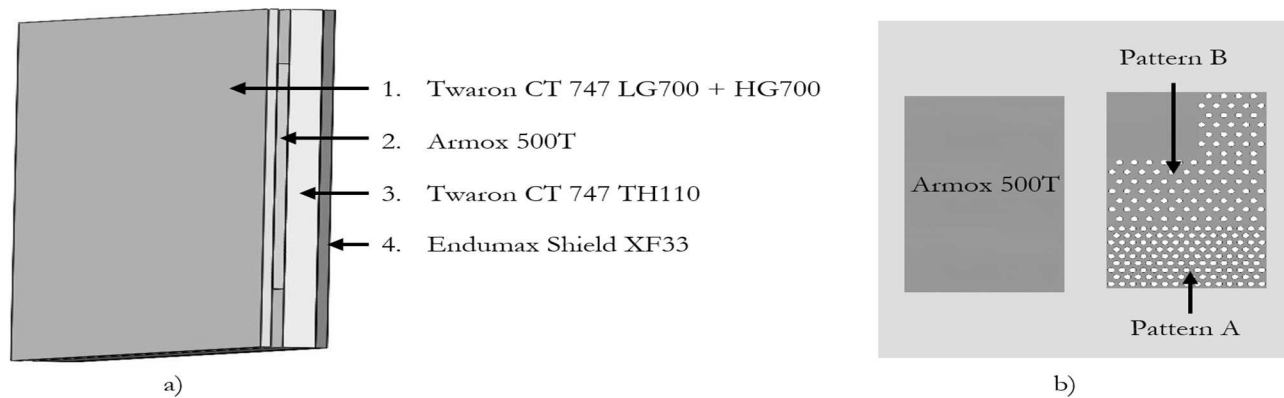
Fig. 12 *Assembled model of the test multi-layered composite armour: a) assembly of the multi-layered composite armour Armox-Aramid-UHMWPE; b) placement of the armour sheets Armox 500T*

3.2 Ballistic resistance of the designed armour

The ballistic resistance of the assembled multi-layered composite armour Armox-Aramid-UHMPWE, see Figure 12, was tested by the rifle cartridges 7.62 x 51 mm FMJ NATO M80 according to standard STANAG AEP-55 NATO, level 1.

In the first part, the ballistic resistance of the multi-layered composite armour with non-perforated sheet Armox 500T was tested. The total weight was 3.89 kg with the thickness of 34.2 mm. Two projectiles 7.62 mm FMJ M80 were fired into the armour. The armour was not penetrated. After the impact of these projectiles, only the minor plastic deformation appeared in the rear part. Fig. 13 shows the visual location of the impacts and the plastic deformation of the rear side of the tested armour.
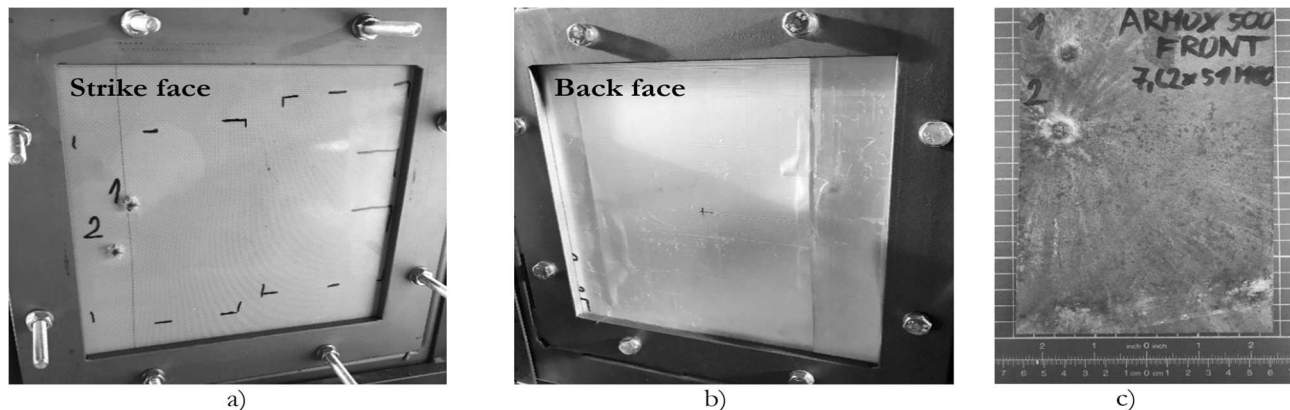

Fig. 13 *Multi-layered composite armour Armox-Aramid-UHMPWE with non-perforated sheet Armox 500T: a) front side of armour; b) rear side of armour; c) projectile impact points into non-perforated sheet Armox 500T*

To reduce the area weight in order to maintain ballistic resistance, the multi-layered composite armour was reinforced with perforated sheet Armox 500T with pattern A. The weight of this armour was 3.61 kg with the thickness of 34.2 mm. This armour was ballistically tested with one projectile 7.62 mm FMJ M80. During the ballistic testing the armour was not penetrated. The projectile stopped at approximately the 8th layer of the composite panel Endumax Shield XF33.

In addition, this armour was ballistically tested with perforated sheet Armox 500T with pattern B. The weight of the armour with pattern B was 3,74 kg. The multi-layered composite armour with perforated sheet, pattern B was completely penetrated during testing. The front and back of the armour after impact of this projectile is shown in Fig. 14. Fig. 15 shows

details of the impacting projectile 7.62 mm FMJ M80, which penetrated the multi-layered composite armour with pattern B.
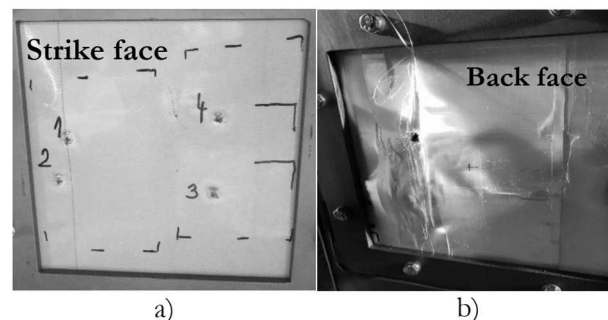

Fig. 14 *Multi-layered composite armour Armox-Aramid-UHMPWE with perforated sheet Armox 500T: a) front side of the armour; b) rear side of the armour*
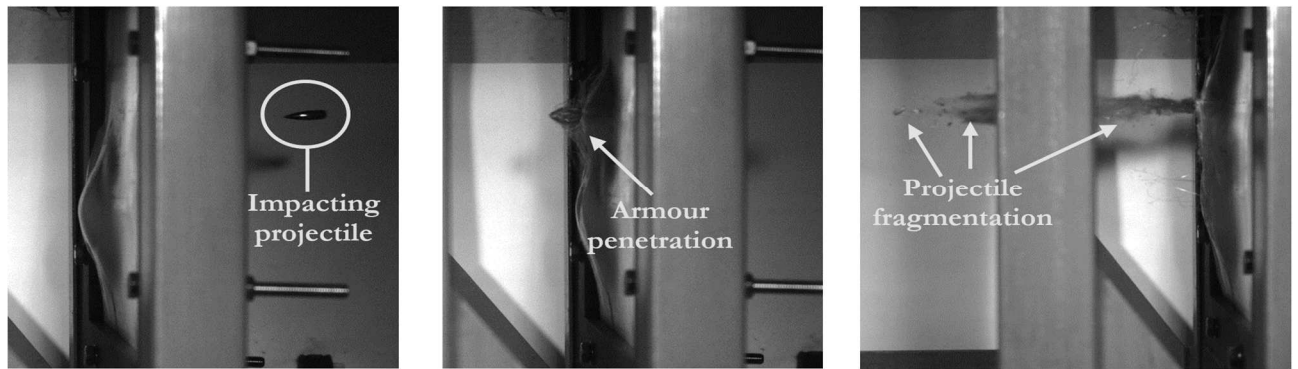
Fig. 15 *High-speed camera images: a) impacting projectile 7.62 mm FMJ M80; b) penetration of armour Armox-Aramid-UHMPWE; c) fragmentation of the projectile*

In the case of the projectile impacting vertically at the midpoint between the four holes of the perforated sheet Armox 500, pattern A, cracks were occurred between the adjacent holes due to the bending stress of this projectile. This stress caused by the bending of the projectile exceeded the strength limit and shear displaced part of the perforated sheet. When the projectile impacted the perforated area with pattern B, the projectile interacted only with the edge of the hole, see Fig. 16. Fig. 16 shows the detail of the damaged area with pattern A and the detail of the damaged area with pattern B. The position of the projectile impact site subsequently determined the failure modes of this sheet.
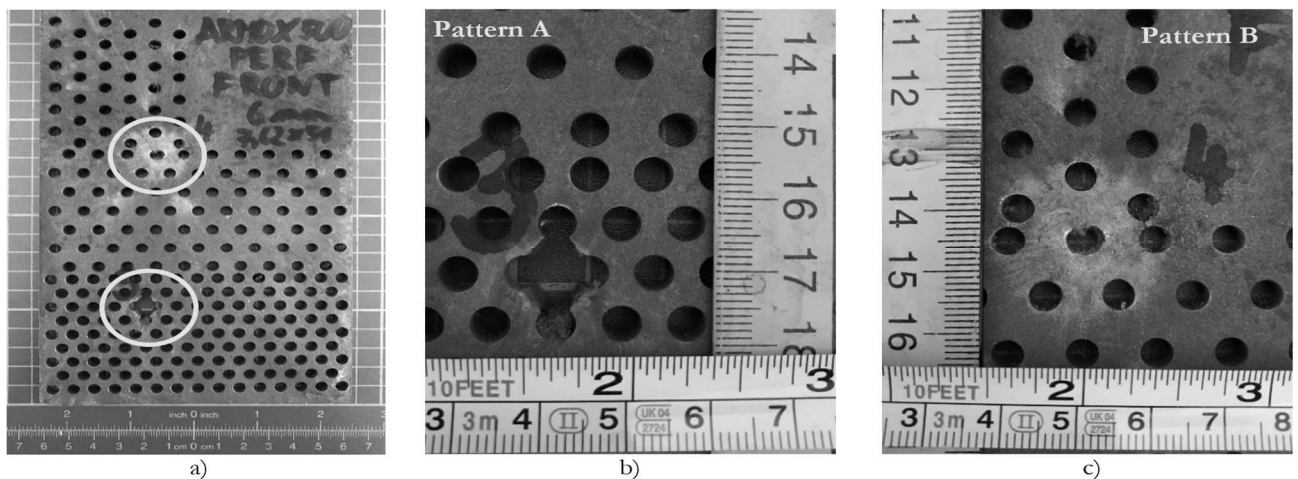

Fig. 16 *Projectile impact into perforated sheet Armox 500T: a) impact location of projectile 7.62 mm FMJ M80; b) pattern damage A; c) pattern damage B*
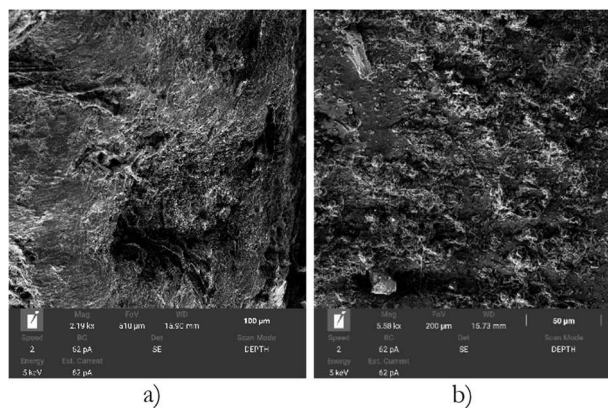

Fig. 17 *Fracture surfaces of Armox 500T, scanning electron microscopy: a) perforated sheet Armox 500T, pattern A (magnified 2000x); b) perforated sheet Armox 500T, pattern A (magnified 5000x)*

To observe the fracture surfaces of perforated sheet Armox 500T with pattern A and B, the scanning electron microscope TESCAN MIRA 4 was used. The fracture surfaces of patterns A and B are shown in Fig. 17.

Fig. 17 shows that there is no significant plastic deformation around the fracture surface. The failure mode was due to tensile stress followed by shear failure. The majority of the fracture surface was characterized by brittle fracture. The appearance of the fracture surface at the point of contact with the projectile consisted of a dimpled pitted microrelief.

During the perforation process in the shooting testing of the designed multi-layered composite armour, the composite panels Twaron CT 747, LG700+HG700, Twaron CT 747 TH110 and Endumax Shield XF33 were dominated by large-scale

delamination in which the individual layers were separated. The most significant damage occurred on the opposite side of the composite panels. During the perforation process, the fibres of the supporting reinforcement were compressed and stretched, while simultaneously bend deformation and shear breaks occurred. The characteristic shape of the damaged panel when the projectile impacted was the conical deformation. Fig. 18 and Fig. 19 show more detailed images of the composite panel damage.
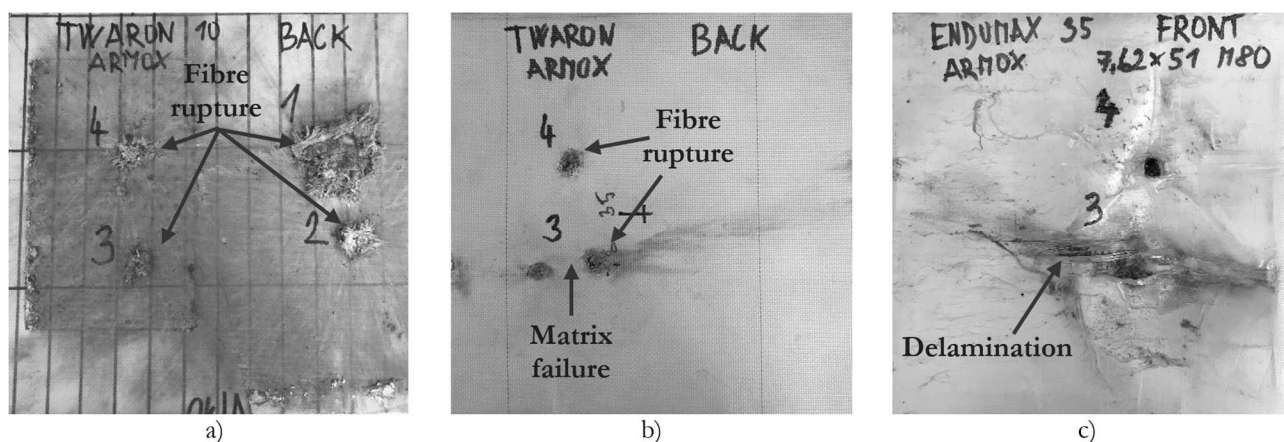

Fig. 18 *Damage mechanisms of ballistic composite panels: a) Twaron CT 747 LG700 + HG700; b) Twaron CT 747 TH110; c) Endumax Shield XF33*
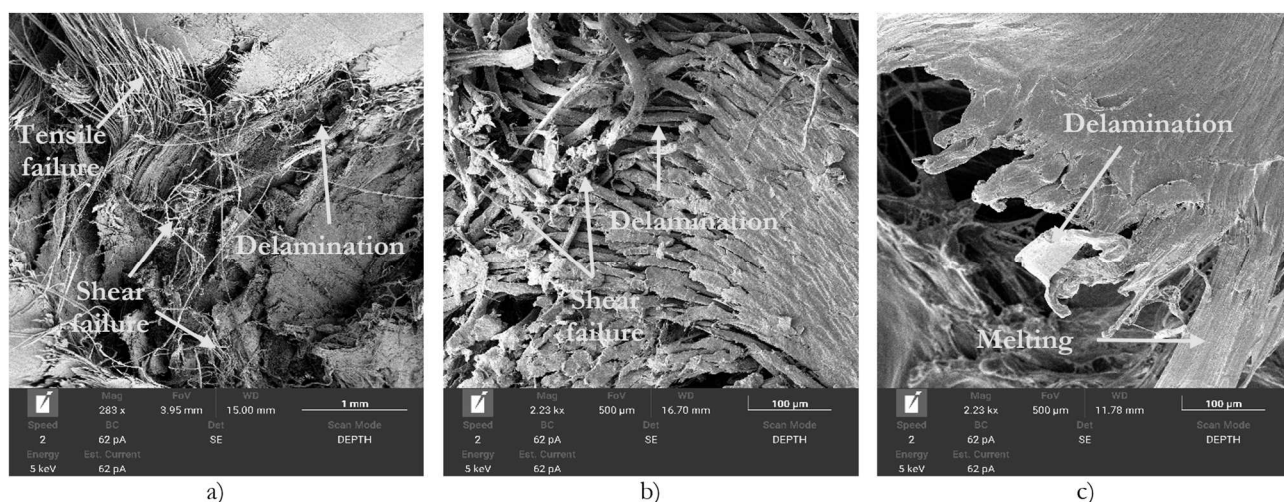

Fig. 19 *Damage mechanisms of ballistic composite panels, scanning electron microscopy: a) Twaron LG700 + HG700 (magnified 200x); b) Twaron CT 747 TH110 (magnified 2000x); c) Endumax Shield XF33 (magnified 2000x)*

The summary of the results from the shooting experiment is shown in Tab. 6. Tab. 6 shows the velocities of the projectiles 7.62 mm FMJ M80 (v_0, v_{25} and v_{0out}) recorded by the ballistic radar (Prototype-ZM, DRS-01) and the corresponding kinetic energies of these projectiles (E_{K0}, E_{K25}, and E_{Kout}).

Tab. 6 *Summary of the results from the shooting experiment*

S. n.	Armour con-figuration	v_0 [m/s]	v_{25} [m/s]	v_{out} [m/s]	E_{K0} [J]	E_{K25} [J]	E_{Kout} [J]	Penetration
1	Unperforated	847.7	821.9	0	3431.3	3225.6	0	No
2	Unperforated	846.5	821.1	0	3421.6	3219.3	0	No
3	Pattern A	863.8	834.5	0	3562.9	3325.3	0	No
4	Pattern B	851.6	828.3	337.1	3462.9	3276.1	542.6	Yes

4 Conclusion

In this study, the ballistic resistance of the designed and fabricated multi-layered composite armour, which was reinforced with non-perforated and perforated sheet Armox 500T, was investigated. The ballistic resistance of the armour Armox-Aramid-UHMWPE was tested according to STANAG AEP-55 NATO, level 1 by the projectile 7.62 mm FMJ M80.

Through the wide-ranging composite materials research, production technologies and ballistic testing, the following conclusions were reached:

- The test configuration, see Fig. 12, was designed according to the measured hardness data of the sheet Armox 500T and the composite materials Twaron CT 747 and Endumax Shield XF33. The hardness results obtained for the composite materials, see Fig. 11, are significantly influenced by the processing technology of the composite panels.

- The proposed configuration was reinforced with non-perforated sheet Armox 500T. The total weight of the test configuration with the non-perforated sheet was 3.89 kg. This configuration was not penetrated after projectile impact and minor plastic deformation in the rear part was exhibited. The main disadvantage was the high weight of the armour.

- In order to reduce the area weight, the multi-layered composite armour was reinforced with perforated sheet Armox 500T. Patterns A and B were formed in the different arrangement with the circular holes, see Fig. 5. The weight of the armour with pattern A showed the 7.8 % lower weight than the weight of the armour with the non-perforated sheet Armox 500T. Pattern A showed the 10,9 % lower mass than pattern B. From the experimental results, the sheet Armox 500T with pattern A, see Fig. 16, effectively reduced the weight of the test configuration and absorbed all the kinetic energy of the projectile 7.62 mm FMJ M80. Pattern B, which contains less number of interconnected circular holes, resulted in complete penetration of the multi-layered composite armour, see Fig. 15, and does not comply with the ballistic resistance according to STANAG AEP-55 NATO, level 1.

- The damage mechanisms of the perforated sheet and composite materials were evaluated after the impact of the projectile 7.62 mm FMJ M80 into the multi-layered composite armour. For the perforated sheet, brittle fracture induced by cleavage was predominant. For the composite materials, delamination of the layers dominated and stretching and shear rupture of the fibres occurred.

The designed multi-layered composite armour with Armox 500T reinforcing perforated plate with pattern A shows considerable potential in terms of reducing the area weight and maintaining ballistic resistance. Numerical simulations for subsequent optimisation should be used in the evaluation of the multihit resistance of this armour with reinforcing perforated sheet Armox 500T.

Acknowledgement

References

[1] ROLC, S., BUCHAR, J., KŘESŤAN, J., KRÁTKÝ J., ŘÍDKÝ R. (2022). *Pancéřová ochrana.* Praha: Academia. Gerstner. ISBN 978-80-200-3100-6.

[2] NOVAK, L., CORNAK, S. (2015). A contribution to shooting resistance evaluation of military vehicles. In *International Conference on Military Technologies* (ICMT) 2015, pp. 1-4. IEEE. https://doi.org/10.1109/MILTECHS.2015.7153711

[3] CHEESEMAN, B. A., BOGETTI, T. A. (2003). Ballistic impact into fabric and compliant composite laminates. *Composite Structures*, 61(1-2), 161-173. https://doi.org/10.1016/S0263-8223(03)00029-1

[4] POKORNÝ, Z., KADLEC, J., HRUBÝ, V., JOSKA, Z., TRAN, D. Q., BERAN, D. (2022). Plasma Nitriding of Bored Barrels. *Advances in*

Military Technology, Vol. 6, No. 1, pp. 69–76. Retrieved from https://aimt.cz/index.php/aimt/article/view/1616

[5] BHATNAGAR, A. (2016). Lightweight Ballistic Composites, Military and Law-Enforcement Applications, 2nd ed.; *Woodhead Publishing*: Cambridge, UK. ISBN 978-0-08-100406-7.

[6] POKORNY, Z., STUDENY, Z., POSPICHAL, M., JOSKA, Z., HRUBY, V. (2015). Characteristics of Plasma Nitrided Layers. *Manufacturing Technology*, Vol. 15, No. 3, pp. 403-409. https://doi.org/10.21062/ujep/x.2015/a/1213-2489/MT/15/3/403

[7] CROUCH, I. G. (2019). Body armor – New materials, new systems. *Defence Technology*, Vol. 15, No. 3, pp. 241-253. https://doi.org/10.1016/j.dt.2019.02.002

[8] DEMIR, T., ÜBEYLI, M., YILDIRIM, R. O. (2008). Investigation on the ballistic impact behavior of various alloys against 7.62mm armor piercing projectile. *Materials and Design*, Vol. 29, No. 10, pp. 2009-2016. https://doi.org/10.1016/j.matdes.2008.04.010

[9] GÖDE, E., TEOMAN, A., ÇETIN, B., TONBUL, K., DAVUT, K., KUŞHAN, M. C. (2023). An experimental study on the ballistic performance of ultra-high hardness armor steel (Armox 600T) against 7.62 mm × 51 M61 AP projectile in the multi-hit condition. *Engineering Science and Technology, an International Journal*, Vol. 38. https://doi.org/10.1016/j.jestch.2023.101337

[10] RANAWEERA, P., BAMBACH, M. R., WEERASINGHE, D., MOHOTTI, D. (2023). Ballistic impact response of monolithic steel and tri-metallic steel–titanium–aluminium armor to nonrigid NATO FMJ M80 projectiles. *Thin-Walled Structures*, Vol. 182. https://doi.org/10.1016/j.tws.2022.110200

[11] ABTEW, M. A., BOUSSU, F., BRUNIAUX, P. (2021). Dynamic impact protective body armor: A comprehensive appraisal on panel engineering design and its prospective materials. *Defence Technology*, Vol. 17, No. 6, pp. 2027-2049. https://doi.org/10.1016/j.dt.2021.03.016

[12] DODDAMANI, S., KULKARNI, S. M., JOLADARASHI, S., T S, M. K., GURJAR, A. K. (2023). Analysis of light weight natural fiber composites against ballistic impact: A review.

International Journal of Lightweight Materials and Manufacture, Vol. 6, No. 3, pp. 450-468. https://doi.org/10.1016/j.ijlmm.2023.01.003

[13] VILIŠ, J., POKORNÝ, Z., ZOUHAR, J. (2022). TESTING THE BALLISTIC RESISTANCE OF COMPOSITE MATERIALS. In: *31st International Conference on Metallurgy and Materials, METAL 2022*. Ostrava: TANGER Ltd., pp. 656-661. ISSN 2694-9296. ISBN 978-1-7138-6230-7. doi:10.37904/metal.2022.4436

[14] POSPÍCHAL, M., DVOŘÁKOVÁ, R., STUDENÝ, Z., POKORNÝ, Z. (2015). Influence of Initial Carbon Concentration on Nitride Layers. *Manufacturing Technology*, Vol. 15, No. 5, pp. 889-893. https://doi.org/10.21062/ujep/x.2015/a/1213-2489/MT/15/5/889

[15] PROCHAZKA, J., POKORNY, Z., JASENAK, J., MAJERIK, J., NEUMANN, V. (2021). Possibilities of the Utilization of Ferritic Nitrocarburizing on Case-Hardening Steels. *Materials*, Vol. 14, No. 13. https://doi.org/10.3390/ma14133714

[16] VILIŠ, J., POKORNÝ, Z., ZOUHAR, J., VÍTEK, R., PROCHÁZKA, J. (2022). Evaluation of ballistic resistance of thermoplastic and thermoset composite panels. *Journal of Physics: Conference Series*, Vol. 2382, No. 1. https://doi.org/10.1088/1742-6596/2382/1/012024

[17] STUDENY, Z., DOBROCKY, D., VILIŠ, J., ADAM, J. (2022). Overview of tribological properties of UHMW polyethylene under rotation. *Journal of Physics: Conference Series*, Vol. 2382, No. 1. https://doi.org/10.1088/1742-6596/2382/1/012013

[18] VILIŠ, J., POKORNÝ, Z., ZOUHAR, J., JOPEK, M. (2022). Ballistic Resistance of Composite Materials Tested by Taylor Anvil Test. *Manufacturing Technology*, Vol. 22, No. 5, pp. 610-616. https://doi.org/10.21062/mft.2022.074

[19] Twaron CT 747. Teijin Limited. *Ballistic Materials Handbook* [online]. Japan: Tokyo, Osaka. Teijin-Aramid-Ballistic-handbook.pdf (teijinaramid.com)

[20] Endumax Shield XF33. Teijin Limited. *Ballistic Materials Handbook* [online]. Japan: Tokyo, Osaka. https://www.teijinaramid.com/wp-content/uploads/2018/12/18033TEI-Prod-broch-Endumax_LR.pdf

[21] Armox® 500T, SSAB. Datasheet Armox® 500T. Available online: https://www.ssab.com/en/brands-and-products/armox/product-offer/armox-500t

[22] HASHIM, N., MAJID, D. L., UDA, N., ZAHARI, R., YIDRIS, N. (2017). Vacuum infusion method for woven carbon/Kevlar reinforced hybrid composite. *IOP Conference Series: Materials Science and Engineering*, Vol. 270. https://doi.org/10.1088/1757-899X/270/1/012021

[23] MA, Y., WANG, J., ZHAO, Y., WEI, X., JU, L., CHEN, Y. (2020). A New Vacuum Pressure Infiltration CFRP Method and Preparation Experimental Study of Composite. *Polymers*, Vol. 12, No. 2. https://doi.org/10.3390/polym12020419

[24] ISO 6507-1. Metallic materials - Vickers hardness test - Part 1: Test method.

[25] ISO 48-4. Rubber, vulcanized or thermoplastic elastomer - Determination of hardness - Part 4: Hardness by the indentation method (Shore hardness).

[26] NIJ STANDARD-0101.06. Ballistic Resistance of Body Armor. National Institute of Justice: Washington, DC, USA.

[27] ČSN 39 5360. Zkoušky odolnosti ochranných prostředků – Zkoušky odolnosti proti střelám, střepinám a bodným zbraním- Technické požadavky a zkoušky. Praha: Česká agentura pro standardizaci, 2018.

[28] VPAM APR 2006. General basis for ballistic material, construction and product testing: Requirements, test levels and test procedures. Rijswijk: Association of test laboratories for bullet resistant materials and constructions. https://www.vpam.eu/pruefrichtlinien/aktuell/apr-2006/

[29] ČOS 130027. Balistická odolnost osobních ochranných prostředků při ohrožení střepinami – modifikovaná metoda. Praha: Úřad pro obrannou standardizaci, katalogizaci a státní ověřování jakosti, 2022. https://oos-data.army.cz/cos/cos/130027.pdf

[30] STANAG 2920 Edition 1. NATO - Military Agency for Standardization (MAS) Ballistic Test Method for Personal Armor Materials and Combat Clothing. NATO Standardization Agency. Brussels, Belgium.

[31] NATO, AEP-55, STANAG 4569. Protection levels for occupants of logistic and light armored vehicles. Part 1-4: General – Annex A", First edition, Volume 1. Brussels, Belgium.